

## Searches for vector-like leptons in ATLAS

---

**Shalini Epari<sup>a,\*</sup> for the ATLAS collaboration**

<sup>a</sup>*Institut de Física d'Altes Energies (IFAE),  
Edifici Cn, Campus UAB, Bellaterra (Barcelona), Spain,*

*E-mail:* [shalini.epari@cern.ch](mailto:shalini.epari@cern.ch)

Vector-like leptons (VLLs) are among the simplest extensions of the Standard Model, with masses near the TeV scale. Depending on the assumed  $SU(2)$  representation, VLLs can appear either as an  $SU(2)$  doublet or singlet in the model. The latest results on searches for VLLs from the ATLAS Collaboration are presented in this talk, probing final states with multiple leptons, jets, and missing transverse energy. No evidence for new physics is observed and 95% confidence level limits are placed on the mass of vector-like electrons and muons appearing as  $SU(2)$  singlets and vector-like taus appearing as  $SU(2)$  doublets.

*12<sup>th</sup> Edition of the Large Hadron Collider Physics Conference  
3-7 June 2024  
Boston, USA*

---

\*Speaker



## 1. Introduction

There are multiple hints of physics beyond the Standard Model (SM) with no clear answers. Among the simplest extensions of the SM at the electroweak scale are vector-like fermions, whose left- and right-handed chiral components have the same transformation properties under the weak-isospin  $SU(2)$  gauge group. These particles arise in many UV-complete BSM models, are expected to have mass close to the TeV scale, mix with SM fermions and provide an explanation to the flavor puzzle [1, 2], or even a dark matter candidate [3]. A broad search program has been developed for vector-like quarks [4] at the ATLAS experiment [5]. On the other hand, VLLs are only recently gaining interest. Compared to vector-like quarks, these searches are challenging because VLLs are expected to be produced via the electroweak interaction and thus, have much lower production cross-sections. Models containing these particles might explain the observed tensions between the measured and predicted values of the anomalous moment of the muon [6] and the *Cabibbo angle anomaly* [7].

The production and decay modes for VLLs depend on the assumed  $SU(2)$  representation [8]. The  $SU(2)$  doublet model consists of an electrically charged and an electrically neutral VLL. The  $SU(2)$  singlet model, on the other hand, consist of just the charged VLLs, with additional couplings that allow decays to SM neutrinos, in addition to charged leptons. The production cross-sections for the doublet model are enhanced by the  $W$ -mediated production modes, which have a much larger cross-section than those mediated by  $Z/\gamma^*$ . The branching ratio of the charged VLL from the doublet model to either the Higgs or  $Z$  boson become equal and plateau at high VLL masses, following the Goldstone boson equivalence theorem. Further, decays to the  $Z$  boson are kinematically favorable at low VLL mass. On the other hand, in the singlet model, the additional  $W$  decay mode is always higher in branching ratio than the decay modes to the Higgs or  $Z$  boson.

These models offer rich phenomenology, characterized by final states involving multiple light leptons, jets, and missing transverse energy, providing a promising avenue for experimental searches at high-energy colliders.

## 2. Search for heavy lepton resonances decaying to a $Z$ boson and a lepton

This is a model-independent search for heavy leptons resonances decaying to a  $Z$  boson and a lepton and an electron or a muon, based on proton-proton collision data taken at 8 TeV by the ATLAS experiment at the CERN Large Hadron Collider, corresponding to an integrated luminosity of  $20.3 \text{ fb}^{-1}$  [9]. The results are interpreted in the context of vector-like electrons (VLL $e$ ) and vector-like muons (VLL $\mu$ ) from an  $SU(2)$  singlet, and type-III seesaw models. The results for the former models are discussed in this talk. Figure 1 shows the Feynman diagram of interest for the VLL interpretation.

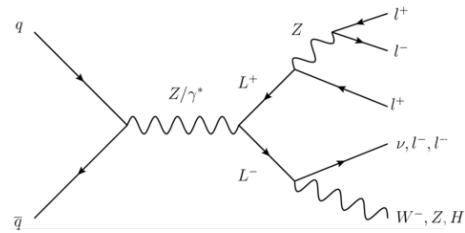


**Figure 1:** Feynman diagram illustrating the pair production and decay of vector-like electrons or muons from an  $SU(2)$  singlet [9].

Events with three high-transverse-momentum electrons or muons are selected, where exactly one lepton pair is compatible with a boson decay and the third lepton is collimated with the boson (with  $\Delta R < 3$ ). To maximize sensitivity, signal regions are split according to the flavor of the additional lepton, shown in Figure 2:

- $Z + e$  regions target VLL $e$ :  $3l + jj$  (targeting a  $W \rightarrow qq$  candidate),  $3l -$  ‘only’ (no  $W \rightarrow qq$  candidate) and  $4l$ .
- $Z + \mu$  regions target VLL $\mu$ :  $3l + jj$  (targeting a  $W \rightarrow qq$  candidate),  $3l -$  ‘only’ (no  $W \rightarrow qq$  candidate) and  $4l$ .

The search aims to identify a narrowly peaked excess in the invariant mass distribution  $\Delta m = m_{3l} - m_{l+l-}$ . Major backgrounds, such as diboson production, are validated in dedicated control regions, including regions with off-shell bosons, high transverse momentum ( $p_T$ ), and specific lepton flavor combinations.

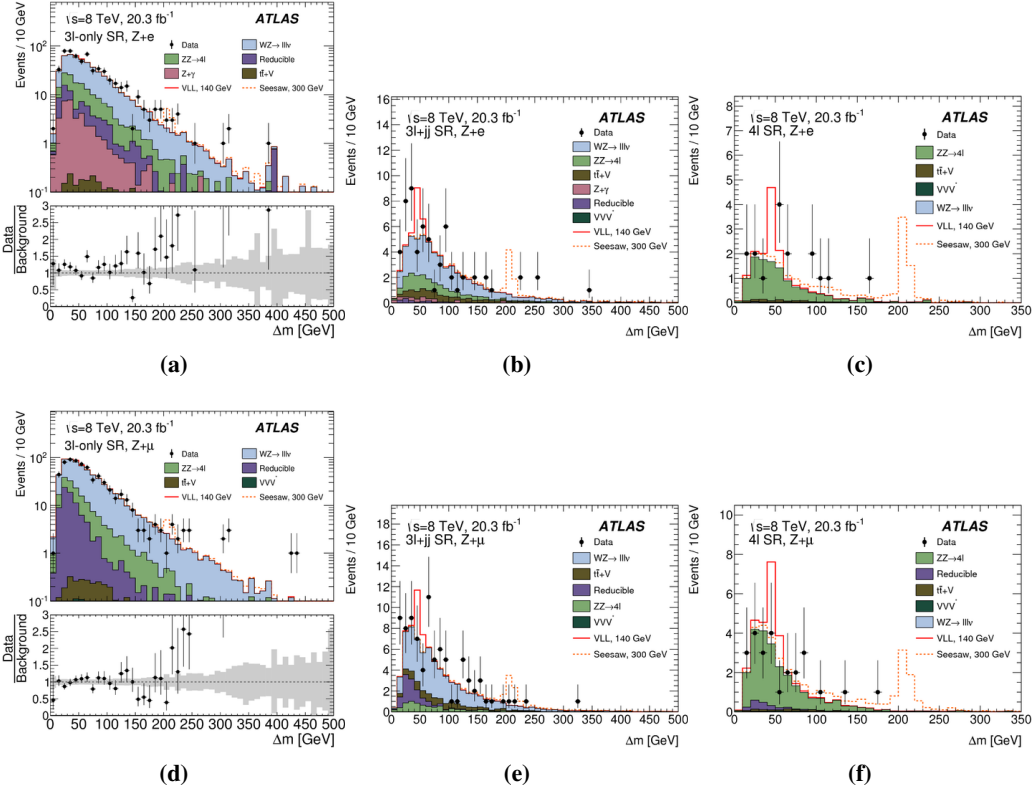


**Figure 2:** Distributions of  $\Delta m = m_{3l} - m_{l+l-}$  in the (a-c)  $Z + e$  regions targeting VLL $e$  signals and (d-f)  $Z + \mu$  regions targeting VLL $\mu$  signals. The error bars on the data points (black) represent statistical uncertainties, and the shaded bands represent the systematic uncertainties on the background predictions [9].

Separate maximum likelihood fits to the data was performed in the  $Z + e$  and  $Z + \mu$  regions for each signal mass hypothesis, including normalization factors for major backgrounds. No significant excess above SM background predictions is observed, and 95% confidence level upper limits on the production cross section of high-mass triplepton resonances are derived, shown in Figure 3. The

search excluded  $VLL_e$  from an  $SU(2)$  singlet in the mass range of 129–176 GeV, except 144–163 GeV.  $VLL_\mu$  from an  $SU(2)$  singlet were excluded in the mass range of 114–168 GeV, except 153–160 GeV. While the search was statistically limited, it sets the strictest limits to date on the mass of VLLs from these models.

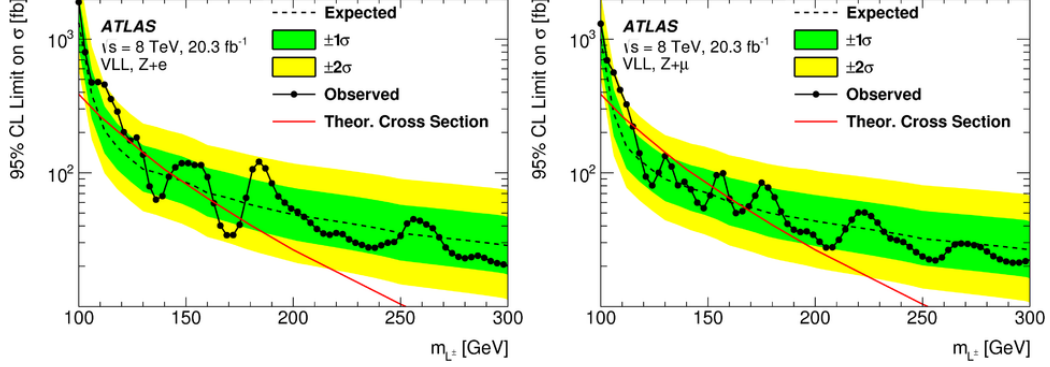


**Figure 3:** The 95% confidence level exclusion limit on the charged VLL production cross section as a function of the VLL mass, from the  $Z + e$  (left) and  $Z + \mu$  (right) regions. The black dashed line represents the expected limit while the shaded regions are its one and two standard-deviation uncertainty bands. The solid black line is the observed limit as a function of VLL mass. The red curve is the leading order theory prediction along with its uncertainty [9].

### 3. Search for third generation vector-like leptons from an $SU(2)$ doublet

This is a search for third generation VLLs in multilepton (two, three, or four-or-more electrons plus muons) final states with zero or more hadronically decaying tau leptons ( $\tau_{\text{had}}$ ) [10]. The search is performed using a dataset corresponding to an integrated luminosity of  $139 \text{ fb}^{-1}$  of  $pp$  collisions at a center-of-mass energy of 13 TeV recorded by the ATLAS detector at the LHC. The Feynman diagrams of interest are shown in Figure 4.

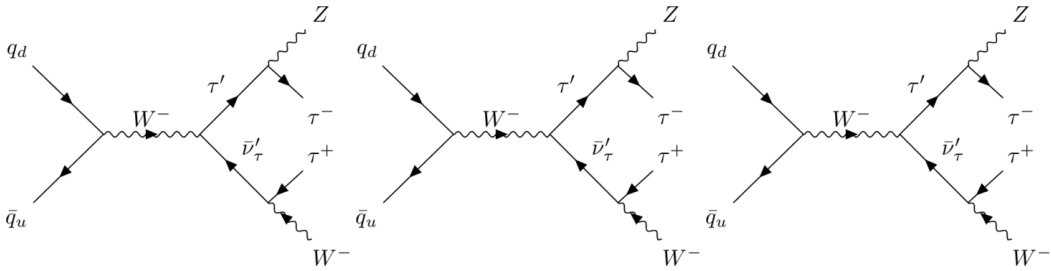


**Figure 4:** Feynman diagrams illustrating the pair production and decay of third generation vector-like leptons from an  $SU(2)$  doublet [10].

The charged and neutral VLLs are assumed to be mass-degenerate [8]. A boosted decision tree (BDT) is employed to maximize signal efficiency while rejecting background events in each of the phase spaces, split according to the light lepton multiplicity, charge, flavor, the number of  $\tau_{\text{had}}$  and missing transverse energy, defined in Table 5a. High BDT score regions serve as the signal regions, while inverting the BDT cut is used for validation or control, defined in Tables 5b and 5c.

A state-of-the-art recurrent neural network (RNN) is used to identify  $\tau_{\text{had}}$  candidates, suppressing the contribution from quarks and gluons misidentified as  $\tau_{\text{had}}$  candidates.

Variables	BDT Training Regions						
BDT	$2\ell$ SSSF, $1\tau$	$2\ell$ SSOF, $1\tau$	$2\ell$ OSSF, $1\tau$	$2\ell$ OSOF, $1\tau$	$2\ell, \geq 2\tau$	$3\ell, \geq 1\tau$	$4\ell, \geq 0\tau$
$N_\ell$	2	2	2	2	2	3	$\geq 4$
Charge/flavour	SSSF	SSOF	OSSF	OSOF	-	-	-
$N_\tau$	1	1	1	1	$\geq 2$	$\geq 1$	$\geq 0$
$E_T^{\text{miss}}$ [GeV]	$\geq 120$	$\geq 90$	$\geq 60$	$\geq 100$	$\geq 60$	$\geq 90$	$\geq 60$

(a)

Variables	Signal Regions						
BDT	$2\ell$ SSSF, $1\tau$	$2\ell$ SSOF, $1\tau$	$2\ell$ OSSF, $1\tau$	$2\ell$ OSOF, $1\tau$	$2\ell, \geq 2\tau$	$3\ell, \geq 1\tau$	$4\ell, \geq 0\tau$
BDT Score	$\geq 0.15$	$\geq 0.1$	$\geq 0.1$	$\geq 0.1$	$\geq -0.11$	$\geq 0.08$	$\geq 0.08$

(b)

	Control Regions				Validation Regions		
	$t\bar{t}+Z$	WZ	ZZ	Fake $\tau_{\text{had}}$	$t\bar{t}+Z$	WZ	ZZ
BDT	$4\ell, \geq 0\tau$	$3\ell, \geq 1\tau$	$4\ell, \geq 0\tau$	$2\ell$ OSSF, $1\tau$	$3\ell, \geq 1\tau$	$2\ell$ SSOF, $1\tau$	$3\ell, \geq 1\tau$
$N_\ell$	$\geq 4$	3	$\geq 4$	2	3	2	3
$N_\tau$	$\geq 0$	0	$\geq 0$	1	$\geq 1$	1	$\geq 1$
$N_b$	$> 0$	0	0	-	$> 0$	0	0
$E_T^{\text{miss}}$ [GeV]	$\geq 60$	$\geq 90$	$< 60$	$\geq 60$	-	-	-
Charge/flavour	-	-	-	OSSF	-	SSOF	-
BDT score	$< 0.08$	$\geq 0.08$	$< 0.08$	$< -0.15$	$< 0.08$	$< 0.1$	$< 0.08$

(c)

**Figure 5:** (a) The regions used in the training and optimization of the BDT, split according to the light lepton multiplicity, charge, flavor, the number of  $\tau_{\text{had}}$  and missing transverse energy. (b) Signal region and (c) control or validation region definitions after applying a BDT score cut on the training regions [10].

A maximum profile likelihood fit to the data was performed, including all signal regions and major backgrounds (such as diboson,  $t\bar{t}$ , and fake  $\tau_{\text{had}}$ ). Signal region distributions after the profile likelihood fit are shown in Figure 6.

No excess of events is observed beyond the SM expectation and 95% confidence level limits are placed on the production cross-section of the VLLs as a function of VLL mass, shown in Figure 7. The search excludes vector-like leptons (VLLs) in the mass range of 130–970 GeV. This search is limited by data statistics.

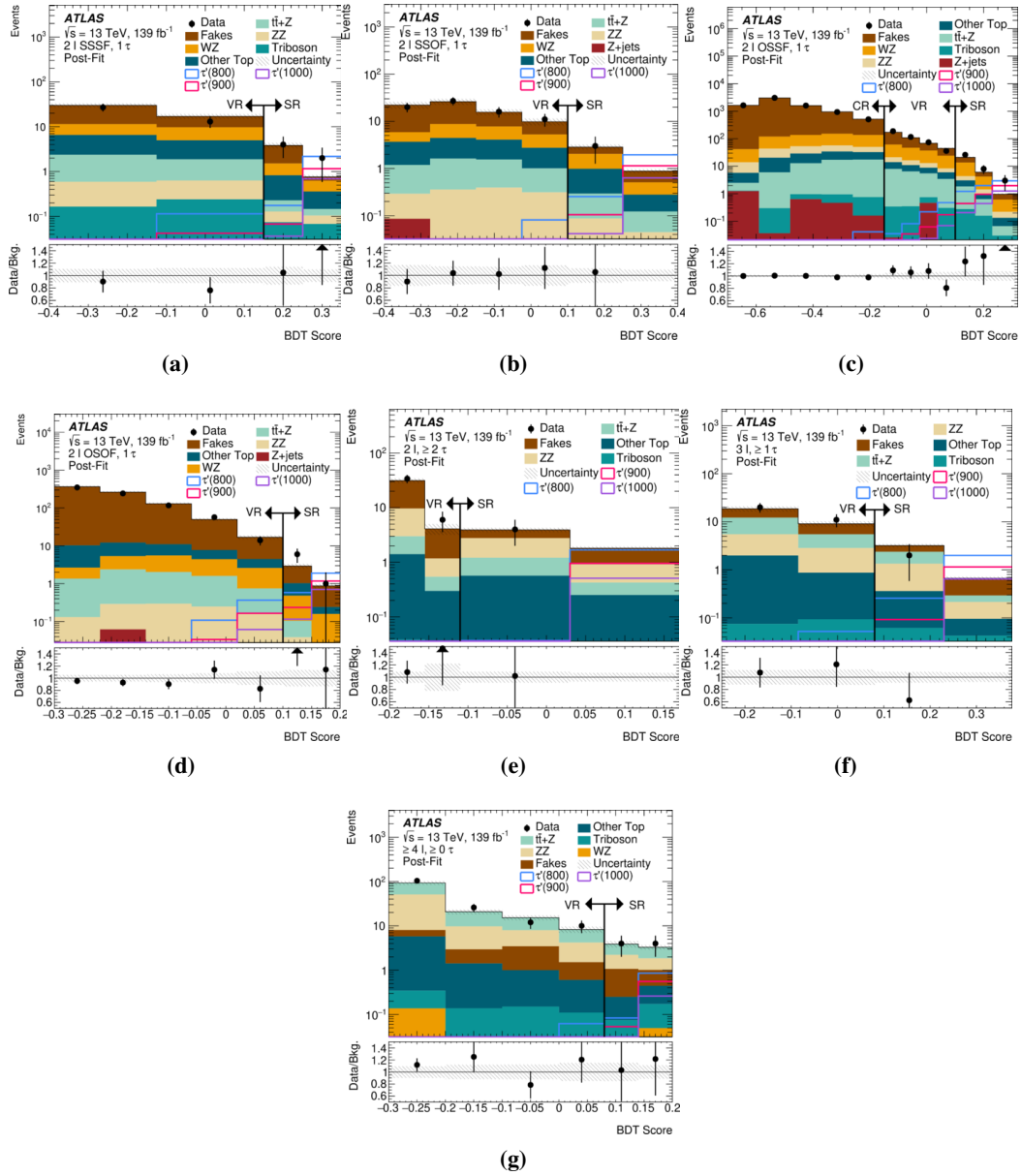


**Figure 6:** BDT score distributions of data and the postfit background in the different BDT training regions (Table 5a). The expected contribution of signal (prefit) is also overlaid. The arrow indicates the SR used in the likelihood fit [10].

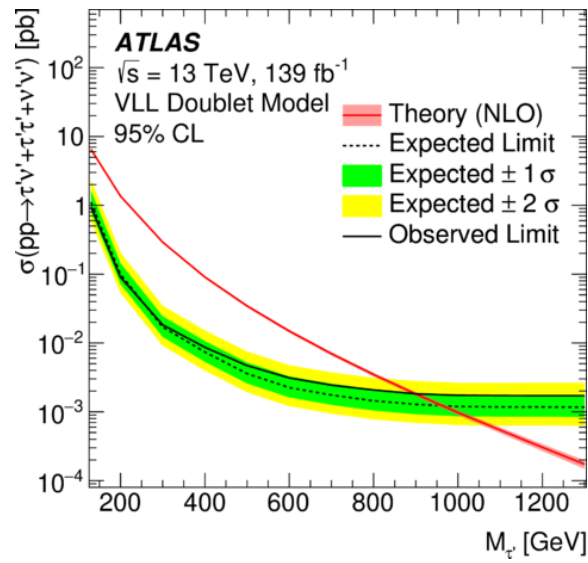


**Figure 7:** The 95% confidence level exclusion limit on the charged VLL production cross section as a function of the VLL mass. The black dashed line represents the expected limit while the shaded regions are its one and two standard-deviation uncertainty bands. The solid black line is the observed limit as a function of VLL mass. The red curve is the next-to-leading order theory prediction along with its uncertainty [10].

## 4. Conclusion

Vector-like lepton searches are a relatively new area of exploration at the LHC. VLLs appear in many ultraviolet (UV) complete models and have the potential to explain several persistent anomalies. This talk presented a broad program of VLL searches performed by the ATLAS Collaboration in Run 1 and Run 2, probing final states with multiple leptons, jets, and missing transverse energy. No evidence for new physics is observed and 95% confidence level limits are placed on the mass of vector-like electrons and muons appearing as  $SU(2)$  singlets and vector-like tau-leptons appearing as  $SU(2)$  doublets.

## References

- [1] Kaustubh Agashe, Takemichi Okui, and Raman Sundrum, *A Common Origin for Neutrino Anarchy and Charged Hierarchies*, Phys. Rev. Lett. **102**, 101801 (2009). doi: [10.1103/PhysRevLett.102.101801](https://doi.org/10.1103/PhysRevLett.102.101801).
- [2] Michele Redi, *Leptons in Composite MFV*, JHEP **09**, 060 (2013). doi: [10.1007/JHEP09\(2013\)060](https://doi.org/10.1007/JHEP09(2013)060).
- [3] Subhaditya Bhattacharya, Purusottam Ghosh, Nirakar Sahoo, and Narendra Sahu, *Mini Review on Vector-Like Leptonic Dark Matter, Neutrino Mass, and Collider Signatures*, Front. in Phys. **7**, 80 (2019). doi: [10.3389/fphy.2019.00080](https://doi.org/10.3389/fphy.2019.00080).
- [4] ATLAS Collaboration, "Exploration at the high-energy frontier: ATLAS Run 2 searches investigating the exotic jungle beyond the Standard Model", CERN-EP-2024-075, <https://arxiv.org/abs/2403.09292> (2024).
- [5] The ATLAS Collaboration et al., "The ATLAS experiment at the CERN Large Hadron Collider", JINST **3**, S08003 (2008).
- [6] D. P. Aguillard *et al.*, *Measurement of the Positive Muon Anomalous Magnetic Moment to 0.20 ppm*, Phys. Rev. Lett. **131**, 161802 (2023). doi: [10.1103/PhysRevLett.131.161802](https://doi.org/10.1103/PhysRevLett.131.161802).
- [7] Andreas Crivellin, Fiona Kirk, Claudio Andrea Manzari, and Marc Montull, *Global Electroweak Fit and Vector-Like Leptons in Light of the Cabibbo Angle Anomaly*, JHEP **12**, 166 (2020). doi: [10.1007/JHEP12\(2020\)166](https://doi.org/10.1007/JHEP12(2020)166).
- [8] N. Kumar and S. P. Martin, "Vectorlike leptons at the Large Hadron Collider," *Physical Review D*, vol. 92, no. 11, p. 115018, Dec. 2015, <http://dx.doi.org/10.1103/PhysRevD.92.115018>.
- [9] ATLAS Collaboration, "Search for heavy lepton resonances decaying to a Z boson and a lepton in pp collisions at  $\sqrt{s} = 8$  TeV with the ATLAS detector," *Journal of High Energy Physics*, 2015, vol. 2015, no. 9, p. 108, [https://doi.org/10.1007/JHEP09\(2015\)108](https://doi.org/10.1007/JHEP09(2015)108).
- [10] ATLAS Collaboration, "Search for third-generation vector-like leptons in pp collisions at  $\sqrt{s} = 13$  TeV with the ATLAS detector," *Journal of High Energy Physics*, 2023, vol. 2023, no. 7, p. 118, [https://doi.org/10.1007/JHEP07\(2023\)118](https://doi.org/10.1007/JHEP07(2023)118).